Journal of
Materials Chemistry B

Materials for biology and medicine

Accepted Manuscript

Journal of
Materials Chemistry B

Materials for biology and medicine

rsc.li/materials-b

Volume 6
Number 3
21 January 2018
Pages 341-528

ISSN 2050-750X

PAPER
Wei Wei, Guanghui Ma et al
Macrophage responses to the physical burden of cell-sized particles

This is an Accepted Manuscript, which has been through the Royal Society of Chemistry peer review process and has been accepted for publication.

Accepted Manuscripts are published online shortly after acceptance, before technical editing, formatting and proof reading. Using this free service, authors can make their results available to the community, in citable form, before we publish the edited article. We will replace this Accepted Manuscript with the edited and formatted Advance Article as soon as it is available.

You can find more information about Accepted Manuscripts in the Information for Authors.

Please note that technical editing may introduce minor changes to the text and/or graphics, which may alter content. The journal's standard Terms & Conditions and the Ethical guidelines still apply. In no event shall the Royal Society of Chemistry be held responsible for any errors or omissions in this Accepted Manuscript or any consequences arising from the use of any information it contains.

ROYAL SOCIETY
OF CHEMISTRY

rsc.li/materials-b

Paper

Disassembling the Complexity of Mucus Barriers to Develop a Fast Screening Tool for Early Drug Discovery

Daniela Peneda Pacheco[a], Cosmin Stefan Butnarasu[b], Francesco Briatico Vangosa[a], Laura Pastorino[c], Livia Visai[d,e], Sonja Visentin[b]*, Paola Petrini[a]*

Mucus is a natural barrier with a protective role that hinders drug diffusion, representing a steric and interactive barrier to overcome for an effective drug delivery to the target sites. In diseases like cystic fibrosis (CF), pulmonary mucus exhibits altered features, which hamper clearance mechanisms and drug diffusion, ultimately leading to lung failure. Effectively modelling the passage through mucus still represents an unmet challenge. An airway CF mucus model is herein proposed to disassemble the complexity of the mucus barrier following a modular approach. A hydrogel, mainly composed of mucin in an alginate (Alg) network, is proposed to specifically model the chemical-physical properties of CF mucus. The steric retention of pathological mucus was reproduced by targeting its mesh size (approximately 50 nm) and viscoelastic properties. The interactive barrier was reproduced by a composition inspired from the CF mucus. Optimized mucus models, composed of 3 mg/ml Alg and 25 mg/ml mucin, exhibited a G' increasing from ~ 21.2 to 55.2 Pa and G" ranging from ~ 5.26 to 28.8 Pa in the frequency range of 0.1 to 20 Hz. Drug diffusion was tested using three model drugs. The proposed mucus model was able to discriminate their mucin-drug interaction and the steric barrier of a mucus layer in respect to the parallel artificial membrane permeability (PAMPA) that models the phospholipidic cell membrane, the state-of-art screening tool for passive drug diffusion. The mucus model can be proposed as *in vitro* tools for early drug discovery, representing a step forward to model the mucus layer. Additionally, the proposed methodology allows to easily include other molecules present within mucus, as relevant proteins, lipids and DNA, and therefore discriminate drug-mucus interactions.

1 Introduction

Mucus is a protective barrier that selectively filters the passage of gases, pathogens, pollutants, and nutrients, and also a barrier for drug products.[1] An effective pharmacological treatment requires that drug products freely diffuse through mucus, otherwise these are eliminated before playing their roles. Drug diffusion through mucus is dependent on its chemical composition, ionic strength, structure and viscoelastic properties, as well as drugs and particles net charge and concentration (Fig. 1).[2] Despite its complex and important role as a barrier, there are no standard protocols that model the mucus barrier. Instead, drug screening platforms typical rely in 2D cell

cultures and parallel artificial membrane permeability (PAMPA) assay. The latter has been adopted to study the permeability of drug products across a lipid-infused artificial membrane. Thus, poor information of possible chemical and steric interactions with mucus has been obtained at the *in vitro* screening stage.[3] This largely affects drug discovering, a long and complex process of about 10 years that includes many stages, the first of which is often called early drug discovery.[4] At this stage, a number of hits requires a fast validation through virtual screening and/or high throughput screening (HTS) to assess possible chemical and structural interactions that determine efficacy and biological performance, and therefore unveil potential drug candidates.[4,5] Often, drug candidates, independently of their target, are compounds expected to pass the mucus.[3] Mimicking the whole complexity of the *in vivo* scenario is a challenge far to be met. Yet, it is now time to provide pharmaceutical companies a standard protocol for the production of relevant mucus models for early drug discovery.

Mucus hypersecretion with altered chemical and structural features has been observed in many diseases as bronchial asthma, chronic obstructive pulmonary disease (COPD), bronchiectasis and cystic fibrosis (CF), whose patients suffer of chronic lung inflammation.[6] CF is a genetic disease that results in the production of thick and viscous mucus secretions in multiple organs. Due to abnormal chloride and HCO_3^- transport and chronic inflammatory states, the CF mucus composition entails a polymeric network made of mucin,[7] albumin[8]

a. Department of Chemistry, Materials and Chemical Engineering "Giulio Natta" at Politecnico di Milano, Milan, Italy
b. Molecular Biotechnology and Health Sciences Department, University of Torino, Torino, Italy
c. Department of Informatics, Bioengineering, Robotics and Systems Engineering, University of Genova, Genova, Italy
d. Molecular Medicine Department (DMM), Center for Health Technologies (CHT), UdR INSTM, University of Pavia, Pavia, Italy
e. Department of Occupational Medicine, Toxicology and Environmental Risks, Istituti Clinici Scientifici Maugeri S.p.A., IRCCS, Pavia, Italy

* Corresponding authors:
Prof. Paola Petrini: paola.petrini@polimi.it
Prof. Sonja Visentin: sonja.visentin@unito.it
Electronic Supplementary Information (ESI) available: [details of any supplementary information available should be included here]. See DOI: 10.1039/x0xx00000x

Paper

and extracellular DNA,[7] increased concentration of calcium (Ca^{2+}) ions,[9] and presence of alginate produced by *Pseudomonas aeruginosa*.[10,11] At the structural level, this pathological chemical cocktail is translated in the presence of a thick (50-400 μm)[9] gel-*like* structure with significantly smaller mesh size (90-190 nm)[12] in respect to physiological mucus (497-503 nm).[13] These molecular interactions generate CF mucus exhibiting shear-thinning behaviour with increased viscosity, storage (*G'*) and loss moduli (*G''*) compared to physiological mucus.[14] Ultimately, drug diffusion and mucus clearance mechanisms are hampered and bacteria find a suitable environment to establish and proliferate that results in lung failure. Different studies have reported chemical binding of different entities to mucin that has direct influence over nanoparticle penetration[15,16] and reduced antibacterial potential of colistin,[17] among others.[18] Sputum - expectorated mass that contains mucus, blood, saliva, among others - is often considered as a first rough *ex vivo* model of CF mucus due to the low invasiveness to retrieve it when compared to physiological mucus. Though, CF sputum possesses contaminants, offers low reproducibility, low stability and time-dependent properties due to both degradation by enzymes present on saliva and molecular disruption by the employed extraction procedure.[19]

Current *in vitro* mucus models used, at the research level, during drug screening either rely on mucin-based solutions or mucin-based structures. Some examples include viscous solutions, as pseudogels, of commercial mucins,[20] mucin solutions mixed with bovine serum albumin[21] and calf thymus DNA,[9] linoleic acid, cholesterol, phosphatidylcholine and pig serum albumin,[22] polyacrylic acid (PAA) gels,[23,24] locust bean gum,[25] and complex mixtures of salmon DNA, egg yolk emulsion, mucin and salts.[26] Another model proposes N-acryloyl-D-glucosamine, a glycopolymer, to model the glycoproteins as that prevalent in mucus – mucins, and 2-hydroxyethylmethacrylate.[27] Yet, mucus-based solutions fail to model the steric barrier of CF mucus, dependent on its mesh size and viscoelastic properties, while those models that reproduce the viscoelastic properties of CF mucus include exogenous compounds that can induce false chemical-physical interactions with drugs and other substances (Table S1).

In our *in vitro* mucus models, we aim to disassemble the complex situation by adopting a modular approach that, when put together, give a more realistic information of drug diffusion through mucus. With this in mind, a mucus model was developed that simplifies the complexity by mimicking the chemical composition, structural features and viscoelastic properties of CF mucus and their impact over drug diffusion was further studied. In this way, a hydrogel composed of mucin and alginate (Alg) – components present in CF mucus - was developed. The viscoelastic properties were modelled by controlling the degree of crosslinking of Alg using Ca^{2+} ions, while the chemical composition was tuned by including mucin, Alg, sodium chloride (NaCl) and Ca^{2+} ions within the range of concentrations reported for CF mucus. The ability of the mucin/Alg hydrogels to model the viscoelastic properties was studied through rheological analysis, whose results were further fitted within the Generalized

Maxwell Model (GMM) aiming at estimating the mesh size of the hydrogels. The mucus model was further coupled to a PAMPA membrane, and its interactive and steric barrier ability was investigated by testing different drugs with different solubility, size, charge at pH 7.4 and reported degree of interaction with mucin.

2   Materials and Methods

2.1   Materials

Mucin from porcine stomach type III (M1778, lot 84082-64-4), sodium salt of alginic acid (Alg, 180947, lot MKBJ0727V), calcium carbonate ($CaCO_3$), D-(+)-gluconic acid δ-lactone ≥99.0% (GDL) and NaCl used to develop the airway mucus model were all purchased from Merck (Germany). All aqueous solutions and suspensions were prepared using distilled water (dH_2O). Potassium phosphate dibasic (K_2HPO_4), potassium phosphate monobasic (KH_2PO_4), and dimethyl sulfoxide (DMSO) were also supplied by Merck to produce the different stability media. Drug diffusion tests were performed using acetylsalicylic acid (CAS# 50-78-2), cephalexin (CAS# 23325-78-2) and epirubicin hydrochloride (CAS# 56390-09-1), which were supplied by Merck.

2.2   Development of an Airway Pathological Mucus Model

Mucin/Alg hydrogels were developed by taking advantage of the internal gelation of Alg by Ca^{2+} ions, in a three-step process. In this way, sodium salt of alginic acid was dissolved at different concentrations (14, 21 and 35 mg/ml) in NaCl solution (16.3 mg/ml), under slow magnetic agitation for 12 hours. In parallel, a mucin solution (43.75 mg/mL) was prepared in dH_2O and left under slow agitation for 12 hours. Both Alg and mucin solutions were mixed at a 1:4 proportion using the double syringe method (step 1). A suspension made of $CaCO_3$ (7 mg/ml) in NaCl solution (16.3 mg/ml) was sonicated (UP200S, Ultrasonic Processor, Hielscher, Ultrasound Technology) for 5 min, centrifuged (Vortex IKA MS3 Orbital Shaker 100-240 V) at 3500 rpm for 1 min, and further mixed with the solution prepared in step 1 in a 1:5 proportion (step 2). Finally, a GDL solution (10 mg/ml) was prepared in NaCl (16.3 mg/mL) and mixed with the solution prepared on step 2 at a proportion of 1:6.

Alg hydrogels were also prepared by substituting the mucin solution by the same volume of dH_2O on step 1, which formulations served as the basis to tailor viscoelastic properties to those of CF sputum, as well as control on the drug diffusion studies to discriminate mucin-drug and possible Alg-drug interactions.

2.3   Physiochemical Characterization

2.3.1   Rheological Characterization

Rheological measurements were performed using a rotational rheometer (AR-1500 TA Instruments, UK) coupled to a cone-plate

Journal of Materials Chemistry B   **Paper**

geometry (diameter: 20 mm, cone angle: 1.023°, truncation 32 μm), at 25°C. First, the linear viscoelastic region of Alg hydrogels was determined by a strain sweep test ranging from 0.1 to 1000%, at an oscillatory frequency of 1 Hz (ω = 2πf = 6.28 rad/s) and was found to be 0.1 – 10%. The storage component (*G', Pa*), and loss component (*G'', Pa*) of the complex modulus (*G*, Pa*), complex viscosity (*η*, Pa.s*) and tan δ (*G''/G'*) of both Alg and mucin/Alg hydrogels were determined through oscillatory frequency sweep measurements. The frequency sweep was performed at a strain amplitude of 1% (accordingly to LVR results), at a logarithmic increasing of frequency set between 0.05 (ω = 0.314 rad/s) and 20 Hz (ω = 125.7 rad/s), to include the ciliary beat frequency (10 – 15 Hz) and breathing rate (0.5 Hz).[28–30] All rheological tests were conducted in triplicate, and Trios Software v3.3 TA Instruments was used for data acquisition and analysis.

2.3.2   Stability Assay

Hydrogels with diameter of 12 mm and thickness of 0.5 mm of each formulation were immersed in different media (4 mL), including dH$_2$O, 1% DMSO, and phosphate buffered saline (PBS, 7.4, composed by 244 g/mL of K$_2$HPO$_4$ and 76 g/ml of KH$_2$PO$_4$). After 24 hours of preparation, stability assessment took place at 25ºC. At pre-determined time points, namely 0.25, 0.5, 1, 2, 4 and 6 hours, each sample was weighted (analytical balance A&D HR-60, USA) and photographed. The weight variation *w(%)* was evaluated as:

$$w(\%) = \frac{w(t) - w(0)}{w(0)} \times 100 \qquad \text{equation (1)}$$

where *w(t)* is the weight of the hydrated sample evaluated after time (*t*) of immersion, and *w(0)* is the initial weight of the respective sample. The photographic images were further processed with ImageJ (32bit) to evaluate the variation in thickness of the sample due to contact with the media. The change of the thickness (h) was determined as:

$$h(\%) = \frac{h(t) - h(0)}{h(0)} \times 100 \qquad \text{equation (2)}$$

where *h(t)* is the thickness of the sample immersed in the medium after time (t) and *h(0)* is the initial thickness prior to immersion.

2.3.3   Drug Diffusion through the Airway Mucus Model

Upon optimization of chemical composition and viscoelastic properties, mucin/Alg hydrogels (Muc/Alg 3) composed by mucin (25 mg/ml) and Alg (3 mg/ml) exhibited superior ability to model the chemical-physical interactions and viscoelastic properties of CF mucus, and therefore was selected as airway mucus model to proceed to the drug diffusion studies. Drug diffusion studies were conducted following the parallel artificial membrane permeability assay (PAMPA; Corning® Gentest™ Pre-coated PAMPA, 353015, USA), with a porosity of 0.45 μm and inner diameter equal to 7.1 mm,

and these were considered as controls to discriminate possible drug-mucus model interactions. Different drugs were tested, including acetylsalicylic acid, cephalexin, and epirubicin. To do so, solutions of acetylsalicylic acid (20 mM), cephalexin (20 mM) and epirubicin (1 mM) were prepared by dissolving the powder in DMSO and subsequently diluted with 2 mM PBS.

Prior to drug diffusion tests, the airway mucus models were produced over the PAMPA membrane, producing a hydrogel of approximately 500 μm in thickness, and left to crosslink for 24 hours. The donor compartment was then filled with the relevant drug solution (200 μl) and its diffusion was evaluated for up to 6 hours. At defined time points, all release media were collected, and an equivalent amount of fresh PBS was added. Optical density of acetylsalicylic acid, cephalexin and epirubicin were measured at 267, 261, and 483 nm, respectively, by UV-vis spectroscopy (Double Beam Spectrophotometer Hitachi UH5300, Japan) and quantified using their relevant calibration curves. The amount of drug released was calculated as follows:

$$\% \ Drug \ Released = \frac{C(t)}{C(0)} \times 100 \qquad \text{equation (3)}$$

where *C(t)* denotes the concentration of drug released at time t and *C(0)* represents the initial concentration introduced on the donor compartment.

The apparent permeability coefficient (Papp) was also calculated according to Equation (4), where dC/dt is the drug permeation rate, *V* is the volume of drug introduced in the donor compartment, *A* is the surface area and *C(0)* represents the initial concentration introduced on the donor compartment.

$$P_{app} = \frac{dC}{dt} \times \frac{V}{A \times C_0} \qquad \text{equation (4)}$$

2.4 Statistical Analysis

The results of at least three independent experiments are presented as mean ± standard deviation (SD). Statistical analysis was performed using the student t-test and ANOVA calculated using GraphPad Prism version 6 (GraphPad Software, USA). Significance differences were set for *$p < 0.05$.

3   Results & discussion

Mucus confers a protective barrier that is selective towards molecules, gases and bacteria. Yet, diseases like bronchial asthma, COPD, bronchiectasis and CF lead to altered viscoelastic properties and chemical compositions, which produce an even stronger barrier towards the diffusion of drugs and particles, and therefore unsuccessful pharmacological treatment. The need to characterize drug behaviour in pathological mucus during drug formulation,

Paper

Journal of Materials Chemistry B

design and optimization has urged the development of mucus models. A mucin/Alg-based airway mucus model that reproduces the chemical-physical properties of CF mucus was developed, envisioned as fast, simple and reproducible tool for pharmacological screening. In this regard, commercial mucin from porcine stomach was selected owing to its structural similarity to tracheobronchial mucins[31], although some differences are present[32]. Commercial mucins are cheaper, easily available, and exhibit higher standardization in respect to laboratory isolated mucins. Owing to the extraction/purification process, commercial mucins are not able to form gels at physiological pH, because these lose their ability to form disulphide bonds[33]. Yet, it has been also reported that *P. aeruginosa* exhibit sulfatase activity, which upon infection enables it to degrade mucins present in CF mucus and further use its by-products as carbon and sulphur sources for growth[34,35]. Therefore, degraded mucins, such as commercial mucins, possibly represent a step forward on modelling the inflammatory situation encountered in pathological conditions, while offering a consistent source to develop mucus models. The concentration of mucin within the mucus model was set at 25 mg/ml, since its concentration in CF mucus has been reported from 11 to 27 mg/ml.[36,37] Taking into consideration the composition of CF mucus, Alg (present in the mucus at a concentration of 0.2-2.5 mg/ml due to *P. aeruginosa* infections[10,11]) was used as base material to tailor the viscoelastic properties of the pathological mucus model. At a first stage, Alg hydrogels were produced by varying the concentration of both Alg and Ca^{2+} ions until comparable viscoelastic properties were attained. Afterwards, mucin was added to the formulation of Alg hydrogels aiming at enhancing its similarity to CF mucus composition. All formulations were prepared within a saline environment (NaCl), which final concentration was set at 7.07 mg/ml as reported in the literature for CF mucus.[38]

3.1 Alginate Hydrogels

Alginate (Alg) hydrogels have long been proposed for drug delivery[39,40] and tissue engineering applications[41,42], as well as bioinks.[43,44] Alg and mucin have been previously mixed to disclose the mechanism of interaction relevant in CF.[45,46] On the basis of this knowledge, we propose the combination of mucin and Alg in a hydrogel to produce models of CF mucus. Alg is a linear anionic polysaccharide formed by the repetition of 1,4-β-D-mannuronate (M) units and α-L-glucuronate (G) residues.[47] Owing to the presence of carboxyl groups, Alg is able to crosslink in the presence of divalent cations, as Ca^{2+} ions, at neutral pH, generating a hydrogel which resultant viscoelastic properties depend on M/G ratio and molecular weight.[47,48] It is well-known that the presence of alginate within CF mucus, increases both storage and loss moduli, and viscosity, which can be partly justified by the high content of Ca^{2+} ions within CF mucus that can further interact with Alg and increase the final viscoelastic properties.[49] Similarly, the concentration of Alg plays a crucial role over the final viscoelastic properties of the mucus model, since its formation is based on the ability of Alg to crosslink in the presence of Ca^{2+} ions.[48] With this in mind, extensive rheological characterization was conducted to assess storage (*G', Pa*) and loss

components (*G'', Pa*), of the complex modulus (*G*, Pa*), tan δ, as well as complex viscosity (*η*, Pa.s*), and further compared to the viscoelastic characterization reported by Yuan *et al.* for CF sputum.[14] Different concentrations of Alg were tested and denominated as Alg 2, Alg 3 and Alg 5, for the sake of simplicity, which correspond to a final Alg concentration of 2, 3 or 5 mg/ml, respectively.

3.1.1 Rheological Characterization

Rheological characterization of hydrogels gives important insights about property-structure relationship, which can be useful to predict and correlate diffusion mechanisms of different molecules, as well as to foresee its impact over clearance mechanisms. The viscoelastic behaviour of a material can be investigated by tan δ, which is defined as the ratio of *G''/G'*. If tan δ > 1, the material has predominant viscous behaviour, while materials with tan δ < 1 predominantly exhibit elastic behaviour.[50] CF mucus exhibits gel-*like* behaviour with a predominant elastic component (tan δ < 1) (Fig. 2a), which means that the ciliary beating stretches the mucus rather than making it flow, resulting in mucus accumulation in the airways.[9] Like CF mucus, all developed Alg hydrogels exhibit tan δ < 1, and therefore predominant elastic behaviour (Fig. 2a) possibly associated to both crosslinking sites and entrapped entanglements.[51]

CF mucus displays a shear-thinning behaviour, meaning that its complex viscosity decreases with increased frequency.[14] All Alg hydrogels showed comparable viscoelastic behaviour with a complex viscosity decreasing with frequency (Fig. 2c and d). The complex viscosity exhibited dependency on Alg concentration. Still, no significant differences were observed between the complex viscosity of Alg 2 and Alg 3 hydrogels and CF sputum at all investigated frequencies (Fig. 2c and d). The variation of *G'* and *G''* with frequency is recognized as the "mechanical spectrum" of the structure. In Alg hydrogels, *G'* is dependent on the balance between Alg and Ca^{2+} ions concentration and the amount of water retained in the mesh, while *G''* depends on the sliding of Alg chains among each other.[52,53] A closer examination at both breathing (~0.5 Hz) and ciliary beating frequencies (~10 Hz), revealed that both Alg 2 and Alg 3 hydrogels better model the viscoelastic features of CF sputum (Fig. 2c and d).[14,28–30,54] Both storage and loss components of the complex modulus were in the same order of magnitude as those reported by Fernández Farréz and co-workers, for Alg hydrogels made of 10 mg/ml Alg, which *G'* ranged from 93.5 to 158 Pa, while *G''* oscillated from approximately 19.5 to 51.9 Pa.[55] Yet, all the developed Alg hydrogels showed a higher value for the complex modulus, *G**, and therefore result stiffer than the CF sputum. This is especially true for Alg 5 hydrogels, which also fail to model *η** and *G'* at breathing rate frequency, as well as *G'* at ciliary beating frequency (Fig. 2c and d).

3.1.2 Stability Assay

The airway mucus model is expected to incorporate a high content of water, between 90-99%, owing to the interaction of Alg with Ca^{2+}

ions that enables both its crosslinking and swelling. Considering that during drug screening, drugs can be dissolved in different media, the stability of the different Alg hydrogels was assessed at 25°C in dH_2O, PBS and 1% DMSO over a period of 6 hours (Fig. 3). Stability was assessed regarding weight and thickness variations, as these are crucial features to guarantee suitable drug testing. After 6 hours, the percentage of weight variation exhibited three distinct behaviours according to the Alg hydrogel composition. When in contact with dH_2O, PBS or 1% DMSO, Alg hydrogels showed that the swelling degree depends on Alg concentration, which not only affects viscoelastic properties, but also hydrogel stability. The decreased percentage weight and thickness of Alg 2 hydrogels might be related to loss of material up to 6 hours incubation, which was also observed on Alg 5 hydrogels immersed in 1% DMSO (Fig. 3a). On the other hand, Alg 5 hydrogels showed increased percentage weight and thickness when incubated in dH_2O and PBS, possible associated to swelling phenomena. Alg 3 hydrogels exhibited superior stability in all media in terms of weight and thickness, when compared to the other Alg hydrogels (Fig. 3).

Increased concentrations of Alg led to an increase of the solid-like characteristic over the viscous behaviour (Fig. 2c) indicating increased crosslinking degree with increased Alg concentrations. By further increasing the concentration of Alg (Fig. S1) this trend is clearly observable. Thus, the hydrogel containing the lowest concentration of alginate was the less stable in all the studied media, with significant decrease of weight and thickness, indicating mass loss, concomitant with a significant decrease of G', indicating the weakening of the structure. This result is consistent with Alg 2 being the less crosslinked hydrogels (tan δ = 0.165 in respect to 0.123 and 0.103 of Alg 3 and Alg 5 hydrogels, respectively; Fig. 2a). Minimal variations were observed for the intermediate concentrations with a not significative effect on the rheological properties, thus indicating a slight mass loss while retaining the bulk properties (Fig. 3c). A complex situation is observed for Alg 5. Different phenomena may occur during immersion of this hydrogel: the weight and the thickness increase due to the swelling of the hydrogels. The swelling of the hydrogels in water and PBS differs accounting the different ionic strength which equilibrates with the salt contents within the hydrogel. Surprisingly, the G' of the hydrogels is not affected by the increased water content (Fig. 3c).

Mucin/Alginate Hydrogels

3.1.3   Rheological Characterization

Aiming at closely modelling the chemical composition of CF mucus, mucin was added to Alg 2, Alg 3 and Alg 5 hydrogels, at a final concentration of 25 mg/ml. The addition of mucin (Muc/Alg 2, Muc/Alg 3 and Muc/Alg 5 hydrogels) was followed by rheological characterization to analyse possible structural distresses (Fig. 4). The tan δ of the Muc/Alg hydrogels better represented those of CF sputum than Alg hydrogels alone, independently of Alg content (Fig.

4a).[50] The addition of mucin differently impacted the final viscoelastic properties of Muc/Alg hydrogels. The viscoelastic properties of Muc/Alg 2 hydrogels were barely affected by the presence of mucin. Yet, the presence of mucin within Muc/Alg 3 hydrogels resulted in greater G'' (Fig. 4c and d). Finally, Muc/Alg 5 hydrogels presented decreased G*, $\eta*$ and G', which can hint some degree of interaction between mucin and Alg (Fig. 4b, c and d). In Muc/Alg hydrogels, in which the concentration of Alg is 2 or 3 mg/ml, mucin seems to be homogeneously distributed and non-interacting so that, when submitted to deformation, slides on the crosslinked Alg chains. Nevertheless, for Muc/Alg 5 hydrogels, possible electrostatic interactions might have occurred between mucin and the Alg.[45,49] It has been shown that mucin interactions with the carboxyl groups of Alg are promoted by the presence of NaCl, while possible hydrogen bonds and van der Waals interactions associated to the mannuronic acid unit of Alg backbone might occur.[45,46,49,56] This is in accordance to the adhesion studies between alginate and commercial mucins reported by Popeski-Dimovski.[46] Previous studies have also shown that mucin and alginate are able to interact when in solution to form gels. Yet, these studies employ purified mucins, instead of commercial mucins, which retain their ability to interact at physiological conditions.[45,49] However, as previously mentioned, purified mucins are harder to obtain and present interindividual variability that results in varied chemical composition and viscoelastic properties, and therefore they are not suitable for the development of standard mucus models to be routinely adopted by pharmaceutical companies for drug diffusion studies.

Mucus models with viscoelastic properties that match those of pathological mucus were obtained by mimicking the chemical of CF mucus, which incorporate Alg, mucin, NaCl and Ca^{2+} ions. From the viscoelastic point of view, both Muc/Alg 2 and Muc/Alg 3 hydrogels provide viscoelastic properties that match those of CF sputum (Fig. 4). Additionally, the viscoelastic properties of the airway mucus of COPD and asthma patients are comparable to those of CF sputum, and therefore the developed platforms can hold a higher spectrum of applications.[12] Previously, purified pig gastric mucin, DNA and bovine serum albumin were exploited as CF mucus models, though their properties differed in viscoelastic behaviour and magnitude.[9]

Previously developed mucus models rely on the addition of synthetic compounds to tailor the viscoelastic properties to those of CF sputum. A mixture of autoclaved mucin, albumin, DNA, amino acids and pentetic acid have shown similar storage modulus to both Muc/Alg 2 and Muc/Alg 3 hydrogels.[26] Hitherto, pentetic acid is a highly interactive molecule that presents many available interaction sites and is not present in CF sputum. Additionally, no information regarding $\eta*$ and G'' is given, which are important parameters to evaluate diffusion and clearance of mucus. Boegh et al. have also proposed a mucus model composed of PAA, mucin and a lipid/protein mixture, whose rheological properties match the viscoelastic properties of porcine intestinal mucus.[23] Similar results were obtained using locust bean gum as the base material to tailor the viscoelastic properties,[25] but neither locust bean gum nor PAA

are present in the pathological or physiological mucus, which limits their application since these can also contribute to the final steric barrier.

3.1.4 Determination of Mesh Size by Applying the Generalized Maxwell Model (GMM)

The viscoelastic features are associated to crosslinking and entanglement degrees, as well as chemical interaction between the different components present in the structure. Consequently, rheological data can be employed to get information on the mesh size associated to the viscoelastic properties of hydrogels, which can be further correlated to steric hindrance during diffusion processes. The mesh size is defined as the linear distance between two crosslinking sites. The results of frequency sweep analysis of the mucus models were further interpreted in terms of the GMM, which describes the viscoelastic response of the hydrogel as a combination of a series of (elastic) springs and (viscous) dashpot in parallel with an additional spring, as previously described by Turco et al.[57] Both G' and G'' can be modelled as a function of the frequency according to the following equations:

$$G' = G_e + \sum_{i=1}^{n} G_i \frac{(\lambda_i \omega)^2}{1 + (\lambda_i \omega)^2}; G_i = \frac{\eta_i}{\lambda_i} \qquad \text{equation (5)}$$

$$G'' = \sum_{i=1}^{n} G_i \frac{\lambda_i \omega}{1 + (\lambda_i \omega)^2}; G_i = \frac{\eta_i}{\lambda_i} \qquad \text{equation (6)}$$

where n is the number of Maxwell elements considered, G_i, η_i and λ_i represent the spring constant, the dashpot viscosity, and the relaxation time of the i-th Maxwell element, respectively. G_e is the spring constant of the additional spring element. In order to decrease the complexity of fitting, the number of fitting parameters was reduced by imposing that the relaxation time of each subsequent parallel element was 10 times smaller than the preceding one, in agreement with the proposal of Turco et al.[57] Therefore, the parameters of the model are G_e, G_i and λ_1. The GMM was applied to fit the experimental data using five elements (i=5), which minimized the error defined as:

$$err = \sum [(G'_{exp} - G'_{model})^2] \qquad \text{equation (7)}$$

The adoption of GMM allows determining the materials shear modulus after relaxation (G_∞) as:

$$G_\infty = G_e + \sum_{i}^{n} G_i \qquad \text{equation (8)}$$

This corresponds to the shear modulus of a rubbery material and hence, from the Rubber Elasticity Theory, it can be related to the average mesh size (ξ)[57,58] according to the following equation:

$$\xi = \sqrt[3]{\frac{6\beta RT}{\pi N_A G}} \qquad \text{equation (9)}$$

Where β is the front factor (equal to 1 assuming an ideal rubbers models), R, the universal gas constant, T, the absolute temperature, and N_A, the Avogadro constant. The obtained G_∞ and ξ are presented on Table 1 (Fig. S3).

The estimated mesh size by applying the GMM varied accordingly to Alg concentration and presence or absence of mucin (Table 1, Fig. S3). The estimated mesh size decreased with the increasing of Alg concentration. Upon addition of mucin, no significant differences on mesh size were detected for Muc/Alg 3 and Muc/Alg 5 hydrogels, yet Muc/Alg 2 presented greater mesh size upon addition of mucin (Table 1). The shear modulus was found to increase with the concentration of Alg in the presence or absence of mucin ($G_\infty \propto$ Alg concentration$^{0.812}$ and $G_\infty \propto$ Muc/Alg concentration$^{1.89}$), which was also observed for the estimated mesh size ($\xi \propto$ Alg concentration$^{-0.249}$ and $\xi \propto$ Muc/Alg concentration$^{-0.630}$). The obtained magnitudes for the dependency of both shear modulus and mesh size corroborated those reported by Turco et al.[57] The Alg hydrogels developed by Turco et al. displayed different viscoelastic properties than those herein presented, and consequently different mesh size. These differences may be related to higher concentration of Alg and Ca^{2+} ions, as well as the presence of other ions (as divalent ions present in HEPES), which can possibly interact with the Alg backbone and increase crosslinking density, and consequently smaller mesh size (ranging from 3.3 to 5.1 nm dependent on Alg concentration). By applying the described method, Grassi and co-workers estimated that the mesh size of Alg hydrogels ranged from 7.70 to 22.0 nm, accordingly to Alg concentration.[58] Interestingly, Alg 5 hydrogels exhibited a mesh size of about 22.0 nm, which is not far from the Alg 5 hydrogels herein developed (~ 42.9 nm) (Fig. 4). The differences might be explained by the higher Ca^{2+} concentration that the authors employed and therefore higher probability of crosslinking. In a similar fashion, Alg hydrogels produced using 60 mg/ml of CaCl$_2$ displayed an estimated mesh size that range from 1 to 13 nm, from higher (120 mg/ml) to lower (10 mg/ml) Alg concentrations.[59] The smaller mesh size is probably related to high Ca^{2+} concentration and other ions that can be involved on the crosslinking.[57] Additionally, the mesh size estimated for the mucus models herein developed were similar to those reported in the literature for pathological mucus (60 - 300 nm with an average between 90 and 190 nm)[12].

3.1.5 Stability Assay

The stability of Muc/Alg hydrogels was conducted at 25°C in dH$_2$O, PBS and 1% DMSO (Fig. 5). Like Alg 2 hydrogels, Muc/Alg 2 hydrogels present a decreased percentage of both weight and thickness variation either in dH$_2$O or PBS, while Muc/Alg 5 hydrogels showed increased percentage weight variation as observed for Alg 5 hydrogels (Fig. 3a; Fig. 5a). Similarly, Muc/Alg 3 hydrogels presented greater stability in respect to weight and thickness variation (Fig. 5), and therefore proven its applicability at least within 6 hours of experiment.

Rheological analyses were also performed at the end of the 6 hours for the Muc/Alg hydrogels to assess possible degradation (Fig. 5c). As previously observed for Alg 2 hydrogels (Fig. 3c), Muc/Alg 2 hydrogels were also susceptible to incubation in dH_2O and PBS (Fig. 5). The G' of Muc/Alg 2 hydrogels decreased from 21.9 Pa, as prepared, to 3.91 and 2.66 Pa after incubation in dH_2O and PBS, respectively. Interestingly, Muc/Alg 5 hydrogels were also affected by the incubation. In spite of increased weight and thickness after 6 hours of incubation, the G' of these hydrogels decreased from 56.1 Pa as prepared to 29.0 and 26.8 Pa when incubated in dH_2O and PBS, respectively. These corroborates the rheological results, as for Muc/Alg 5 hydrogels decreased $G*$, $\eta*$ and G' was observed in respect to Alg 5 hydrogels, which was hypothesized to be associated to interaction between mucin and Alg (Fig. 4 b, c and d). The decreased G' after incubation might be linked to mucin loss through the incubation period. Muc/Alg 3 hydrogels, in their turn, did not display changes on G' showing their superiority to withstand incubation up to 6 hours (Fig. 5c).

The superior stability combined to its ability to model the viscoelastic properties of pathological airway mucus make Muc/Alg 3 hydrogels the preferred candidate to serve as a platform for drug diffusion studies.

3.2 Drug Diffusion through the Airway Mucus Model

Passive diffusion is the predominant transport phenomenon experienced by drugs aiming at the targeted tissue, and it involves going through both mucus and cell membranes. The diffusion of drugs depends on their permeability through both mucus and the lipid bilayer of epithelial cells. The PAMPA assay is a widely used high-throughput system that contains a lipid-infused artificial membrane and it was adopted, in this study, to simulate the passive transport characteristic of cell membranes. The PAMPA assay presents many advantages, as it is cost-effective, easy- and ready-to-use, it has good reproducibility and good corroboration with the permeability studies conducted using Caco-2 cells, and ensures higher correlation of the obtained results across different laboratories.[60,61] Yet, the PAMPA assay cannot take into consideration the diffusion of drugs through mucus, which is dependent on mucus viscoelastic properties, mesh size, drug-mucin interactions, and drug solubility. In this work, we propose a mucus model that can be easily coupled to the PAMPA membrane to get descriptive information over the steric and interactive effects relevant during drug diffusion through the mucus barrier. Currently, there is no standardized protocol to test drug permeability across lung mucus, which duration differs from study-to-study. Herein, we have studied permeability up to 6 hours, as recent studies focused on the permeation of both drugs and drug delivery systems through CF sputum, porcine intestinal mucus, and intestinal mucus models have been conducted up to 2, 2.5, 4 and 6 hours.[12,23,62–65] As proof of concept, the diffusion of three different drugs, namely acetylsalicylic acid (ASA), cephalexin and epirubicin, was tested across the developed airway mucus model (Muc/Alg 3 hydrogels). The mucus model was prepared over the PAMPA

membrane system, and after crosslinking the different drugs were deposited on top of the mucus model (donor). At specific time points the release medium was collected from the receptor chamber (Fig. 6a). Drug diffusion through the PAMPA membrane was studied as control.

Mucin-drug interactions influence drug pharmacokinetics by reducing drug absorption.[18] In this sense, three different drugs with different degrees of interaction with mucin, dimension, solubility in water, and charge at pH 7.4 were selected (Table 2). In a previous study, it was determined that the K_A of cephalexin shows a moderate interaction with mucin.[18] Following the published method, the K_A of both ASA and epirubicin was evaluated in solution, which revealed low and high interaction, respectively. The obtained original data is presented in Table 2. ASA did not show interaction with mucin, in agreement with what was also observed for mucin solutions (Table 2), and rapidly diffused through the Muc/Alg 3 hydrogels. Its concentration in the receptor chamber after 6 hours was above 90% with no significative differences and a similar diffusion profile (Fig. 6b). In accordance to what was observed in solution, cephalexin was able to interact with the mucin present within the mucus model, and this resulted in a different diffusion profile than that of PAMPA membranes.[18] After 6 hours, the percentage of cephalexin on Muc/Alg 3 hydrogels was 19.5% in comparison to the PAMPA membranes (83.4%; Fig. 6b). Mucin-cephalexin interaction is mainly governed by van der Waals and hydrogen bonds.[18] Our results indicate that this interactive capability is retained by mucin when included in the mucus model. Finally, it was determined that epirubicin shows a strong interaction with mucin in solution (Table 2). Accordingly, in the presence of Muc/Alg 3 hydrogels, the diffusion of epirubicin was strongly hampered with a release of 1.6% in respect to 50.4%, the percentage of drug diffused across the PAMPA membrane (Fig. 6b).

To discriminate the steric effect *versus* the interactive effect, we performed a parallel experiment in Transwell® supports (*i.e.* not employing PAMPA) in which we compared Alg3 hydrogels *versus* Muc/Alg 3 hydrogels (Fig. S4). For ASA, no effects were observed for both hydrogels, indicating no interaction with either mucin or alginate. Cephalexin exhibits a mild interaction with mucin (Table 2) that together with the higher molecular weight compared to ASA, may have played a role in reducing its mobility through both Alg 3 and Muc/Alg 3 hydrogels (Fig. S4). Although, the two hydrogels did not affect in the same way the diffusion (Fig. S4), supporting the hypothesis that van der Walls interactions with mucin, described in solution[18] and observed in the diffusion studies conducted through PAMPA + Muc/Alg 3 hydrogels (Fig. 6), could be involved in slowing down cephalexin diffusion. The high interaction of epirubicin with mucin resulted in a very low amount of epirubicin passing through Muc/Alg 3 hydrogels. The comparison with the diffusion profile of hydrogels composed solely of Alg brings interesting points to discriminate the mucin interaction upon steric interaction. Although Alg 3 hydrogels reduced epirubicin diffusion, the major effects were seen when mucin is present in the model.

To better understand the diffusion profile of the different drugs through the mucus model, a mathematical model was developed based on the convection–diffusion equation (equation 10), in which diffusion force is mainly governed by a concentration gradient (Fig. 6c).

$$\frac{\partial C}{\partial t} = D\nabla^2 - \nabla(C \times v) \qquad\qquad \text{equation (10)}$$

where C is the drug concentration at time t, D is the diffusion coefficient, ∇ is the Laplace operator (which has three coordinates, including x, y and z) and v is the velocity of the mucus model. Different mathematical models have been developed to study drug release from hydrogels when these are applied as drug delivery systems.[66,67] Yet, herein the aim of the developed mathematical model is to study the drug diffusion across the hydrogel, which acts as a barrier.[68] As in this study, the mucus does not move and the drugs only diffuse in x direction of the orthonormal Cartesian reference system, the convection–diffusion equation was simplified into:

$$\frac{\partial c}{\partial t} = D\frac{\partial^2 c}{\partial x^2} \qquad\qquad \text{equation (11)}$$

As boundary conditions it was considered that drug concentration in $x = 0$ (apical layer of the mucus model) changes with time in an exponential manner and the concentration in x equal to thickness is assumed to change as measured in drug diffusion tests and reported in Fig. 6b for each drug. The interpolation function takes into consideration the different behaviour of each drug in the mucus model. As initial conditions it was admitted that at $x = 0$ and $t = 0$ the concentration is equal to $C0$ (initial concentration), while in all the other points (so $x \neq 0$) the concentration is 0 at $t = 0$. By applying the mathematical model, it is possible to assess the topographical drug diffusion profile inside of the mucus model (Fig. 6c). The drug diffusion profile of both ASA and cephalexin is similar, though a slower diffusion was observed for cephalexin, most probably related to its interaction with mucin.[18] The diffusion of epirubicin through the mucus model is extremely slow, with epirubicin retained in the upper layers of the mucus model (Fig. 6c). The nature of this interaction is unknown, although it can be hypothesised that the molecular weight, the high van der Walls area, the positive charge at the considered pH (Table 2) could each play a role or synergistically contribute to the interaction. According to the present results, it is not possible to discriminate which is the determinant characteristic of the strong interaction of this drug with mucin.

4   Conclusions

Aiming at disassembling the complexity of mucus to provide an easy-to-use and easy-to-produce tool, we have developed a viscoelastic hydrogel, with mucin and alginate as major components, to model the compositional and structural

features of mucus for early drug discovery. The mucus model can be easily coupled to state-of-art diffusion models (e.g. PAMPA membranes), expanding their potential to render a more realistic picture of drug diffusion through the mucus barrier. In fact, the proposed model was effective to discriminate both steric and interactive barriers of mucus towards drugs selected for their different chemical-physical and dimensional characteristics.

The mesh size of the hydrogel, estimated by applying the generalized Maxwell model, corroborates the drug diffusion results, giving an insight over the diffusion mechanism. A mathematical model to represent the diffusion was developed to describe the drug diffusion profile through the proposed mucus model. In a broader sense, this set of combined experimental methods and mathematical modelling can be proposed for a deep characterization in the development of hydrogel-based *in vitro* models, whenever the viscoelastic properties, the mesh size, and the diffusion mechanisms are key features to be studied.

It is relevant to highlight that the production method allows to easily incorporate, in a modular approach, other components (*e.g.* albumin, phospholipids, among others) to further recreate the chemical composition of mucus, while allowing to distinguish the contribution of each component over drug diffusion. The proposed mucus model can be exploited as a high throughput screening platform either for cystic fibrosis mucus or other pathological mucus, as mucus of chronic obstructive pulmonary disease, which unveils its potential to a wider range of applications as a fast screening tool for early drug discovery.

Conflicts of interest

There are no conflicts to declare.

Acknowledgements

Notes and references

1   F. Taherali, F. Varum and A. W. Basit, *Adv. Drug Deliv. Rev.*, 2017, **S0169-409X**, 30239–9.

2   A.-C. Groo and F. Lagarce, *Drug Discov. Today*, 2014, **19**, 1097–1108.

3   A. Lechanteur, J. das Neves and B. Sarmento, *Adv. Drug Deliv. Rev.*, 2018, **124**, 50–63.

4   J. Hughes, S. Rees, S. Kalindjian and K. Philpott, *Br. J. Pharmacol.*, 2011, **162**, 1239–1249.

5   E. Lionta, G. Spyrou, D. Vassilatis and Z. Cournia, *Curr. Top. Med. Chem.*, 2014, **14**, 1923–1938.

6   J. V. Fahy and B. F. Dickey, *N. Engl. J. Med.*, 2010, **363**, 2233–2247.

7   V. J. Broughton-Head, J. R. Smith, J. Shur and J. K. Shute, *Pulm. Pharmacol. Ther.*, 2007, **20**, 708–717.

8   N. N. Sanders, E. V. A. N. Rompaey, S. C. D. E. Smedt and J. Demeester, *Crit. Care Med.*, 2001, **164**, 486–493.

9   P. G. Bhat, D. R. Flanagan and M. D. Donovan, *J. Pharm. Sci.*, 1996, **85**, 624–630.

10   C. A. McCaslin, D. N. Petrusca, C. Poirier, K. A. Serban, G. G. Anderson and I. Petrache, *J. Cyst. Fibros.*, 2015, **14**, 70–77.

11   S. M. Kreda, C. W. Davis and M. C. Rose, *Cold Spring Harb. Perspect. Med.*, 2012, **2**, a009589.

12   J. S. Suk, S. K. Lai, Y.-Y. Wang, L. M. Ensign, P. L. Zeitlin, M. P. Boyle and J. Hanes, *Biomaterials*, 2009, **30**, 2591–2597.

13   T. Yu, J. Chisholm, W. J. Choi, A. Anonuevo, S. Pulicare, W. Zhong, M. Chen, C. Fridley, S. K. Lai, L. M. Ensign, J. S. Suk and J. Hanes, *Adv. Healthc. Mater.*, 2016, **5**, 2745–2750.

14   S. Yuan, M. Hollinger, M. E. Lachowicz-Scroggins, S. C. Kerr, E. M. Dunican, B. M. Daniel, S. Ghosh, S. C. Erzurum, B. Willard, S. L. Hazen, X. Huang, S. D. Carrington, S. Oscarson and J. V Fahy, *Sci. Transl. Med.*, 2015, **7**, 276ra27-276ra27.

15   Q. Xu, L. M. Ensign, N. J. Boylan, A. Schön, X. Gong, J.-C. Yang, N. W. Lamb, S. Cai, T. Yu, E. Freire and J. Hanes, *ACS Nano*, 2015, **9**, 9217–9227.

16   N. Barbero, M. Coletti, F. Catalano and S. Visentin, *Int. J. Pharm.*, 2018, **535**, 438–443.

17   J. X. Huang, M. A. T. Blaskovich, R. Pelingon, S. Ramu, A. Kavanagh, A. G. Elliott, M. S. Butler, A. B. Montgomery and M. A. Cooper, *Antimicrob. Agents Chemother.*, 2015, **59**, 5925–5931.

18   C. Pontremoli, N. Barbero, G. Viscardi and S. Visentin, *Bioorg. Med. Chem.*, 2015, **23**, 6581–6586.

19   A. Horsley, K. Rousseau, C. Ridley, W. Flight, A. Jones, T. A. Waigh and D. J. Thornton, *J. Cyst. Fibros.*, 2014, **13**, 260–266.

20   D. A. Norris and P. J. Sinko, *J. Appl. Polym. Sci.*, 1997, **63**, 1481–1492.

21   M. Dawson, E. Krauland, D. Wirtz and J. Hanes, *Biotechnol. Prog.*, 2004, **20**, 851–857.

22   A. W. Larhed, P. Artursson and E. Björk, *Pharm. Res.*, 1998, **15**, 66–71.

23   M. Boegh, S. G. Baldursdóttir, A. Müllertz and H. M. Nielsen, *Eur. J. Pharm. Biopharm.*, 2014, **87**, 227–235.

24   M. Boegh, M. García-Díaz, A. Müllertz and H. M. Nielsen, *Eur. J. Pharm. Biopharm.*, 2015, **95**, 136–143.

25   M. Anwarul Hasan, C. F. Lange and M. L. King, *J. Nonnewton. Fluid Mech.*, 2010, **165**, 1431–1441.

26   Y. Yang, M. D. Tsifansky, C.-J. Wu, H. I. Yang, G. Schmidt and Y. Yeo, *Pharm. Res.*, 2010, **27**, 151–160.

27   M. T. Cook, S. L. Smith and V. V. Khutoryanskiy, *Chem. Commun.*, 2015, **51**, 14447–14450.

28   S. Lum, P. Gustafsson, H. Ljungberg, G. Hulskamp, A. Bush, S. B. Carr, R. Castle, A. -f. Hoo, J. Price, S. Ranganathan, J. Stroobant, A. Wade, C. Wallis, H. Wyatt and J. Stocks, *Thorax*, 2007, **62**, 341–347.

29   H. Wilkens, B. Weingard, A. Lo Mauro, E. Schena, A. Pedotti, G. W. Sybrecht and A. Aliverti, *Thorax*, 2010, **65**, 808–814.

30   D. B. Hill, P. A. Vasquez, J. Mellnik, S. A. McKinley, A. Vose, F. Mu, A. G. Henderson, S. H. Donaldson, N. E. Alexis, R. C. Boucher and M. G. Forest, *PLoS One*, 2014, **9**, e87681.

31   S. L. McGill and H. D. C. Smyth, *Mol. Pharm.*, 2010, **7**, 2280–2288.

32   S. S. Dhanisha, C. Guruvayoorappan, S. Drishya and P. Abeesh, *Crit. Rev. Oncol. Hematol.*, 2018, **122**, 98–122.

33   V. J. Schömig, B. T. Käsdorf, C. Scholz, K. Bidmon, O. Lieleg and S. Berensmeier, *RSC Adv.*, 2016, **6**, 44932–44943.

34   C. V. Robinson, M. R. Elkins, K. M. Bialkowski, D. J. Thornton and M. A. Kertesz, *J. Med. Microbiol.*, 2012, **61**, 1644–1653.

35   J. M. Flynn, D. Niccum, J. M. Dunitz and R. C. Hunter, *PLOS Pathog.*, 2016, **12**, e1005846.

36   M. O. Henke, G. John, M. Germann, H. Lindemann and B. K. Rubin, *Am J Respir Crit Care Med.*, 2007, **175**, 816–821.

37   J. A. Dodge, *Dev Period Med*, 2015, **19**, 9–13.

38   H. Matsui, B. R. Grubb, R. Tarran, S. H. Randell, J. T. Gatzy, C. W. Davis and R. C. Boucher, *Cell*, 1998, **95**, 1005–1015.

39   N. Nikravesh, O. G. Davies, I. Azoidis, R. J. A. Moakes, L. Marani, M. Turner, C. J. Kearney, N. M. Eisenstein, L. M. Grover and S. C. Cox, *Adv. Healthc. Mater.*, 2019, 1801604.

40   R. Zhang, L. Lei, Q. Song and X. Li, *Colloids Surfaces B Biointerfaces*, 2019, **175**, 569–575.

41   B. N. Sathy, A. Daly, T. Gonzalez-Fernandez, D. Olvera, G. Cunniffe, H. O. McCarthy, N. Dunne, O. Jeon, E. Alsberg, T. L. H. Donahue and D. J. Kelly, *Acta Biomater.*, 2019, **88**, 314–324.

42   E. Ruvinov, T. Tavor Re'em, F. Witte and S. Cohen, *J. Orthop. Transl.*, 2019, **16**, 40–52.

43   L. Raddatz, A. Lavrentieva, I. Pepelanova, J. Bahnemann, D. Geier, T. Becker, T. Scheper and S. Beutel, *J. Funct. Biomater.*, 2018, **9**, 63.

44   S. Hafeez, H. Ooi, F. Morgan, C. Mota, M. Dettin, C. van Blitterswijk, L. Moroni and M. Baker, *Gels*, 2018, **4**, 85.

45   C. Taylor, J. Pearson, K. Draget, P. Dettmar and O. Smidsrod, *Carbohydr. Polym.*, 2005, **59**, 189–195.

46   R. Popeski-Dimovski, *Carbohydr. Polym.*, 2015, **123**, 146–149.

47   K. Y. Lee and D. J. Mooney, *Prog. Polym. Sci.*, 2012, **37**, 106–126.

48   B. E. Larsen, J. Bjørnstad, E. O. Pettersen, H. H. Tønnesen and J. E. Melvik, *BMC Biotechnol.*, 2015, **15**, 29.

49   A. Fuongfuchat, A. M. Jamieson, J. Blackwell and T. A. Gerken, *Carbohydr. Res.*, 1996, **284**, 85–99.

50   J.-K. Yan, L.-X. Wu, W.-Y. Qiu, Y.-Y. Wang, Z.-C. Ding and W.-D. Cai, *RSC Adv.*, 2017, **7**, 50441–50448.

51   E. A. Nunamaker, K. J. Otto and D. R. Kipke, *J. Mech. Behav. Biomed. Mater.*, 2011, **4**, 16–33.

52   M. A. LeRoux, F. Guilak and L. A. Setton, *J. Biomed. Mater. Res.*, 1999, **47**, 46–53.

53   C. K. Kuo and P. X. Ma, *Biomaterials*, 2001, **22**, 511–521.

54   S. K. Lai, Y.-Y. Wang, D. Wirtz and J. Hanes, *Adv. Drug Deliv. Rev.*, 2010, **61**, 86–100.

55   I. Fernández Farrés and I. T. Norton, *Food Hydrocoll.*, 2014, **40**, 76–84.

56   B. Menchicchi, J. P. Fuenzalida, A. Hensel, M. J. Swamy, L. David, C. Rochas and F. M. Goycoolea, *Biomacromolecules*, 2015, **16**, 924–935.

57   G. Turco, I. Donati, M. Grassi, G. Marchioli, R. Lapasin and S. Paoletti, *Biomacromolecules*, 2011, **12**, 1272–1282.

58   M. Grassi, C. Sandolo, D. Perin, T. Coviello, R. Lapasin and G. Grassi, *Molecules*, 2009, **14**, 3003–3017.

59   H. B. Eral, V. López-Mejías, M. O'Mahony, B. L. Trout, A. S.

Myerson and P. S. Doyle, *Cryst. Growth Des.*, 2014, **14**, 2073–2082.

60   M. Á. Cabrera-Pérez, M. B. Sanz, V. M. Sanjuan, M. González-Álvarez and I. G. Álvarez, in *Concepts and Models for Drug Permeability Studies*, Elsevier, 2016, pp. 3–29.

61   E. Naderkhani, J. Isaksson, A. Ryzhakov and G. E. Flaten, *J. Pharm. Sci.*, 2014, **103**, 1882–1890.

62   N. N. Sanders, S. C. De Smedt, E. van Rompaey, P. Simoens, F. de Baets and J. Demeester, *Am. J. Respir. Crit. Care Med.*, 2000, **162**, 1905–1911.

63   J. S. Suk, S. K. Lai, N. J. Boylan, M. R. Dawson, M. P. Boyle and J. Hanes, *Nanomedicine*, 2011, **6**, 365–375.

64   H. Friedl, S. Dünnhaupt, F. Hintzen, C. Waldner, S. Parikh, J. P. Pearson, M. D. Wilcox and A. Bernkop-Schnürch, *J. Pharm. Sci.*, 2013, **102**, 4406–4413.

65   F. Lagarce, A.-C. Groo, P. Saulnier, J.-C. Gimel, J. Gravier, C. Ailhas and J.-P. Benoit, *Int. J. Nanomedicine*, 2013, 4291.

66   B. Amsden, *Macromolecules*, 1998, **31**, 8382–8395.

67   D. Caccavo, S. Cascone, G. Lamberti and A. A. Barba, *Mol. Pharm.*, 2015, **12**, 474–483.

68   Y. Cu and W. M. Saltzman, *Adv. Drug Deliv. Rev.*, 2009, **61**, 101–114.

69   PubChem, Aspirin, https://pubchem.ncbi.nlm.nih.gov/compound/2244, (accessed 12 February 2019).

70   PubChem, Cephalexin, https://pubchem.ncbi.nlm.nih.gov/compound/27447, (accessed 12 February 2019).

71   PubChem, Epirubicin, https://pubchem.ncbi.nlm.nih.gov/compound/41867, (accessed 12 February 2019).

72   S. Kirchner, J. L. Fothergill, E. A. Wright, C. E. James, E. Mowat and C. Winstanley, *J. Vis. Exp.*, , DOI:10.3791/3857.
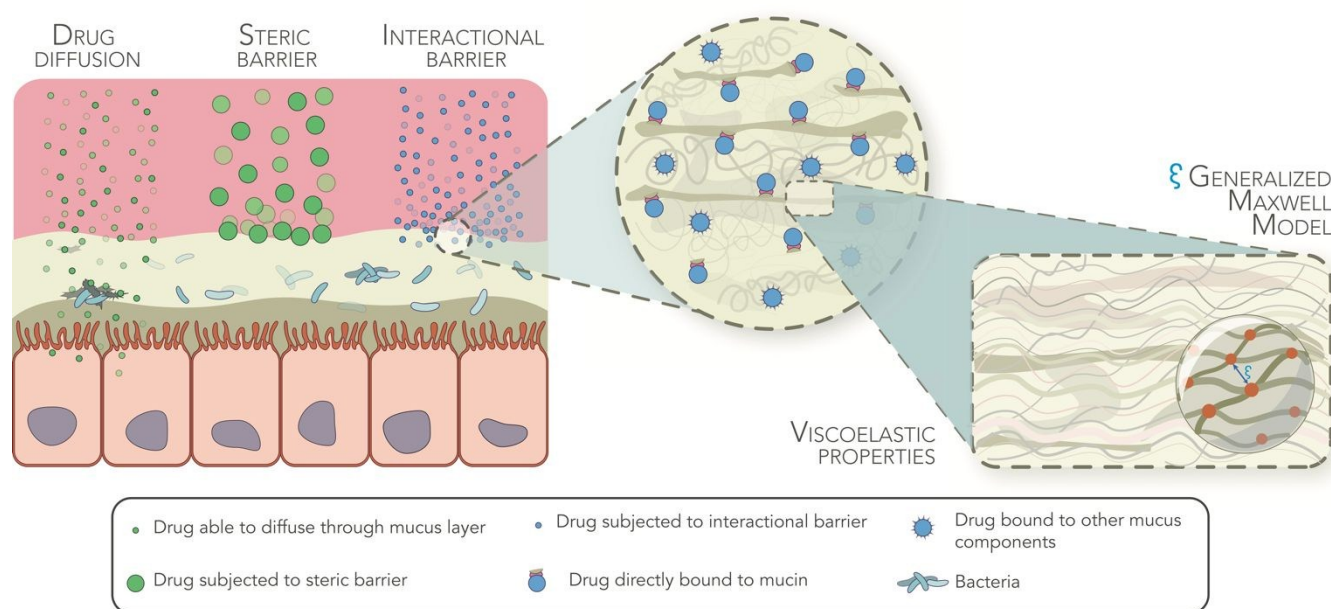
Paper

Fig. 1 Steric and interactive barriers of airway mucus. Particles able to entangle with mucus components are subjected to the interactional barrier of mucus (blue circles, right); diffusion of particles bigger than the size of the mesh between mucin fibbers is hampered by the steric barrier of mucus (green circles, centre); particles not subjected to any of the barriers exposed by mucus freely diffuse through the mucus layer (green circles, left).
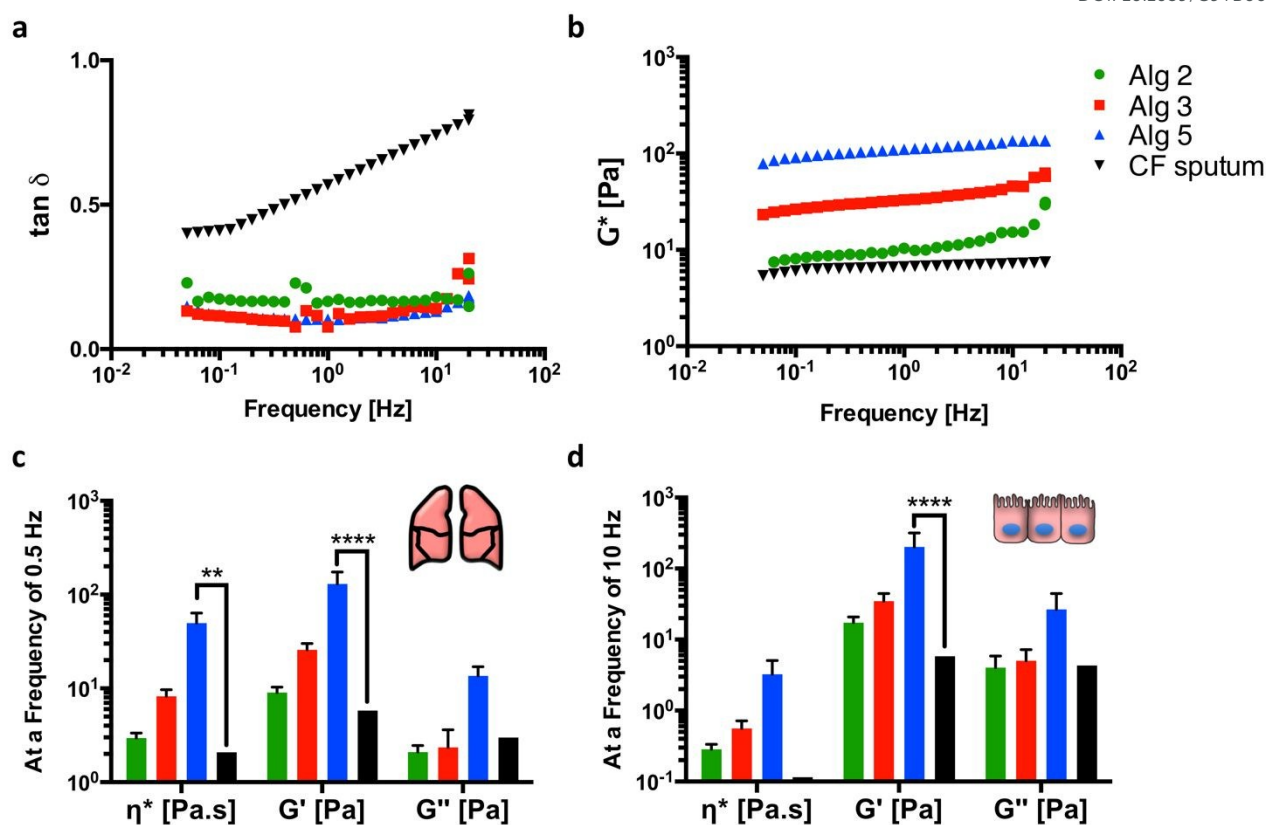
Fig. 2 Rheological characterization in frequency sweep mode of Alg hydrogels and CF sputum. (a) tan δ; and (b) complex modulus (G*, Pa.s).[9,14] η* (Pa.s), G' (Pa) and G'' (Pa) at (c) breathing frequency (~0.5 Hz); and (d) ciliary beating frequency (~10 Hz). Significant differences were set for *p<0.05; **p<0.01; ***p<0.001; ****p<0.0001. Alg 2, Alg 3 and Alg 5 hydrogels are depicted in green, red and blue, respectively, while CF sputum corresponds to black.
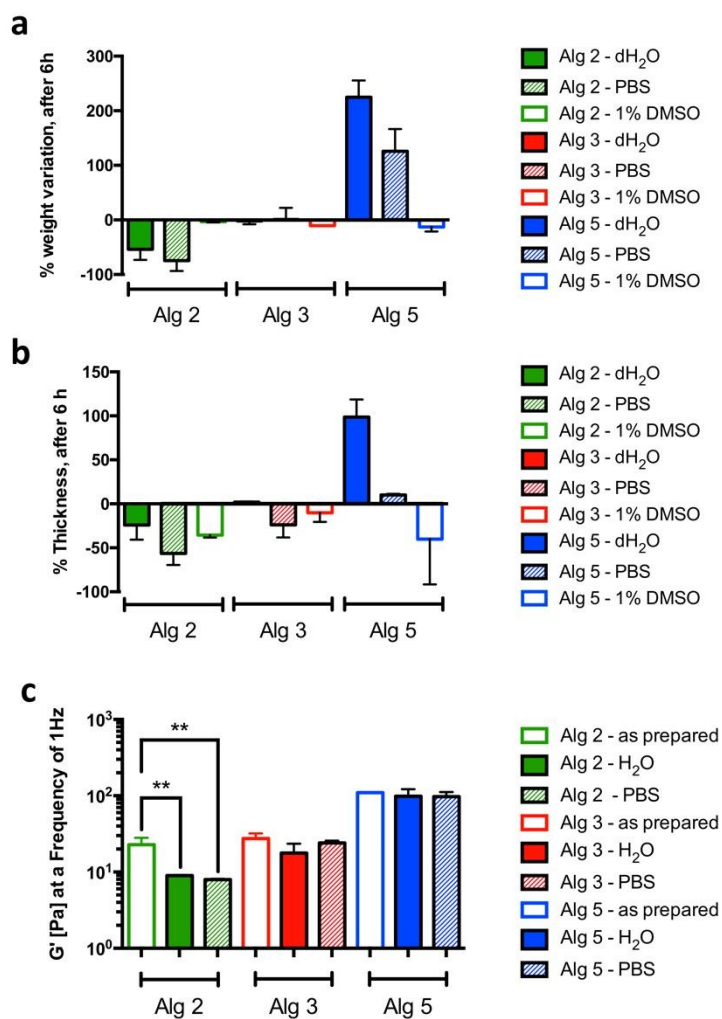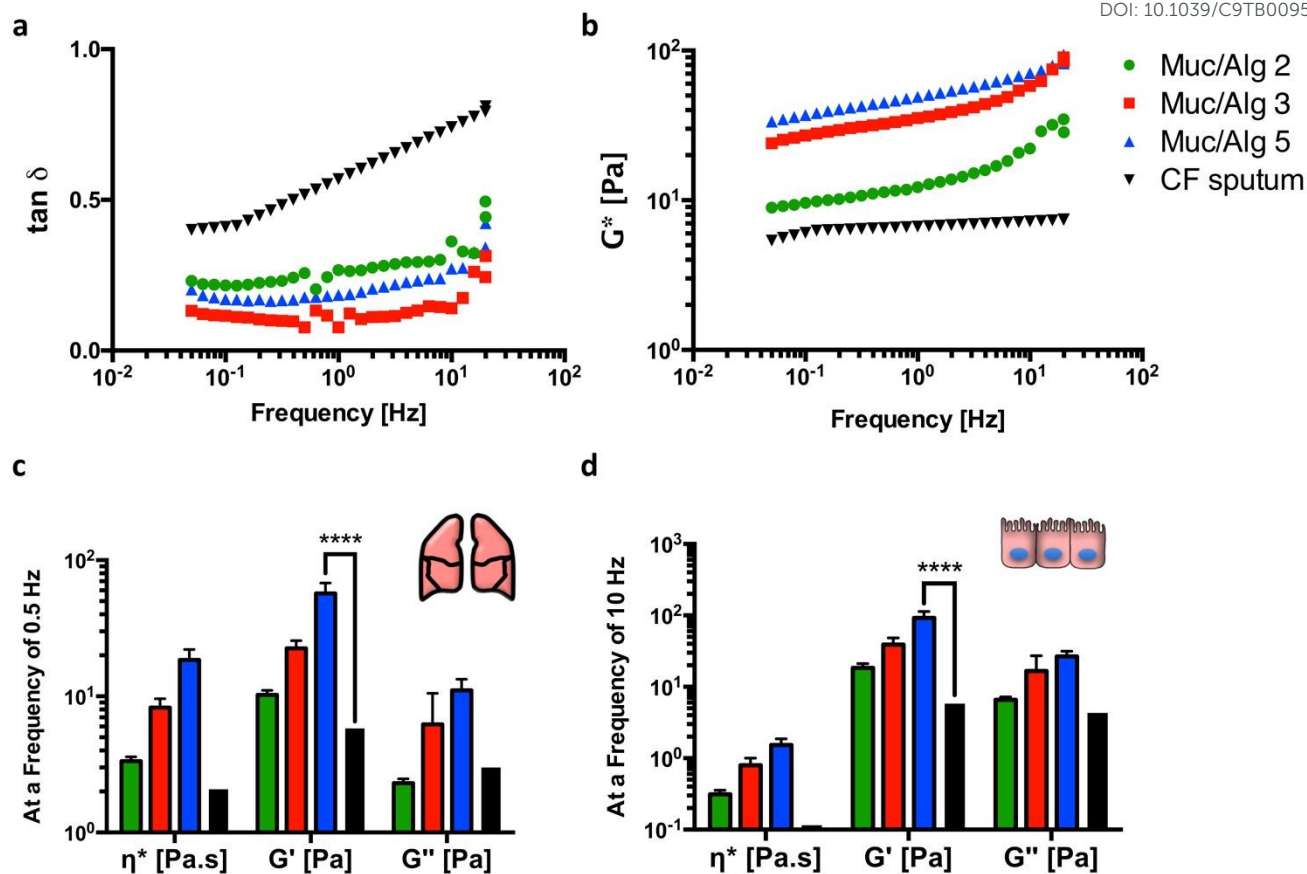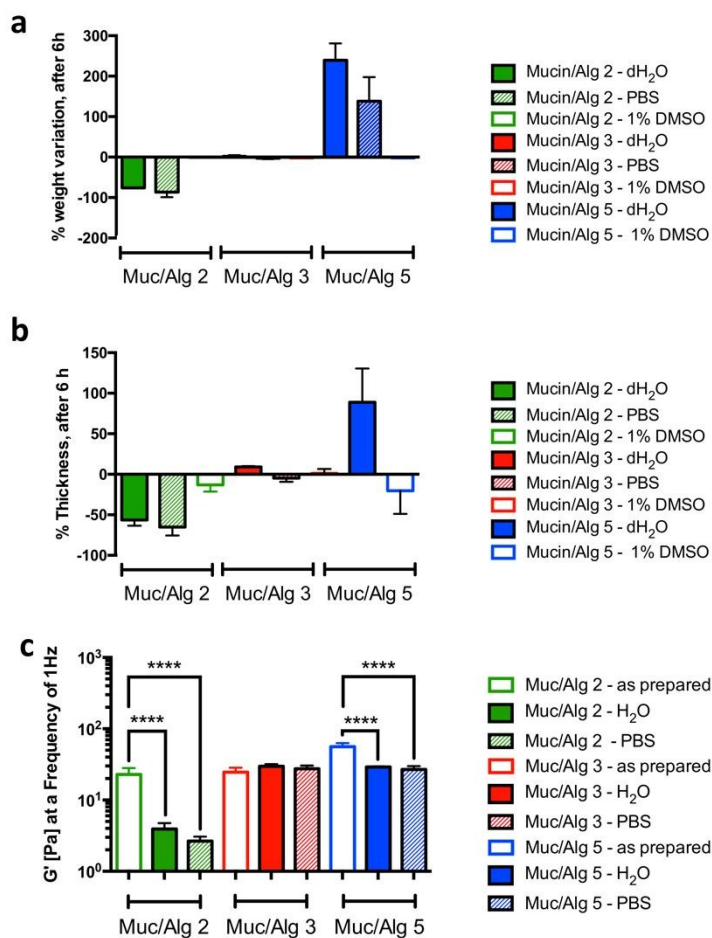
Fig. 3 Stability assessment of different Alg hydrogels. (a) Percentage of weight variation w(%); (b) Percentage of thickness variation h(%); and (c) G' (Pa) on dH_2O, PBS and 1% DMSO, after 6 hours of incubation, at 25°C. Significant differences were set for $*p<0.05$; $**p<0.01$; $***p<0.001$; $****p<0.0001$. Alg 2, Alg 3 and Alg 5 hydrogels are depicted in green, red and blue, respectively.

Fig. 4 Rheological characterization in frequency sweep mode of Muc/Alg hydrogels, Alg hydrogels and CF sputum. (a) tan δ; and (b) Complex modulus (G*, Pa.s).[9,14] η* (Pa.s), G' (Pa) and G'' (Pa) at (c) breathing frequency (~0.5 Hz); and (d) ciliary beating frequency (~10Hz). Significant differences were set for *p<0.05; **p<0.01; ***p<0.001; ****p<0.0001. Muc/Alg 2, Muc/Alg 3 and Muc/Alg 5 hydrogels are depicted in green, red and blue, respectively, while CF sputum corresponds to black.

Fig. 5 Stability assessment of different Muc/Alg hydrogels. (a) Percentage of weight variation (w%); (b) Percentage of thickness variation (h%); and (c) G' (Pa) on dH_2O, PBS and 1% DMSO, after 6 hours of incubation, at 25°C. Significant differences were set for *$p < 0.05$; **$p < 0.01$; ***$p < 0.001$; ****$p < 0.0001$. Muc/Alg 2, Muc/Alg 3 and Muc/Alg 5 hydrogels are depicted in green, red and blue, respectively.
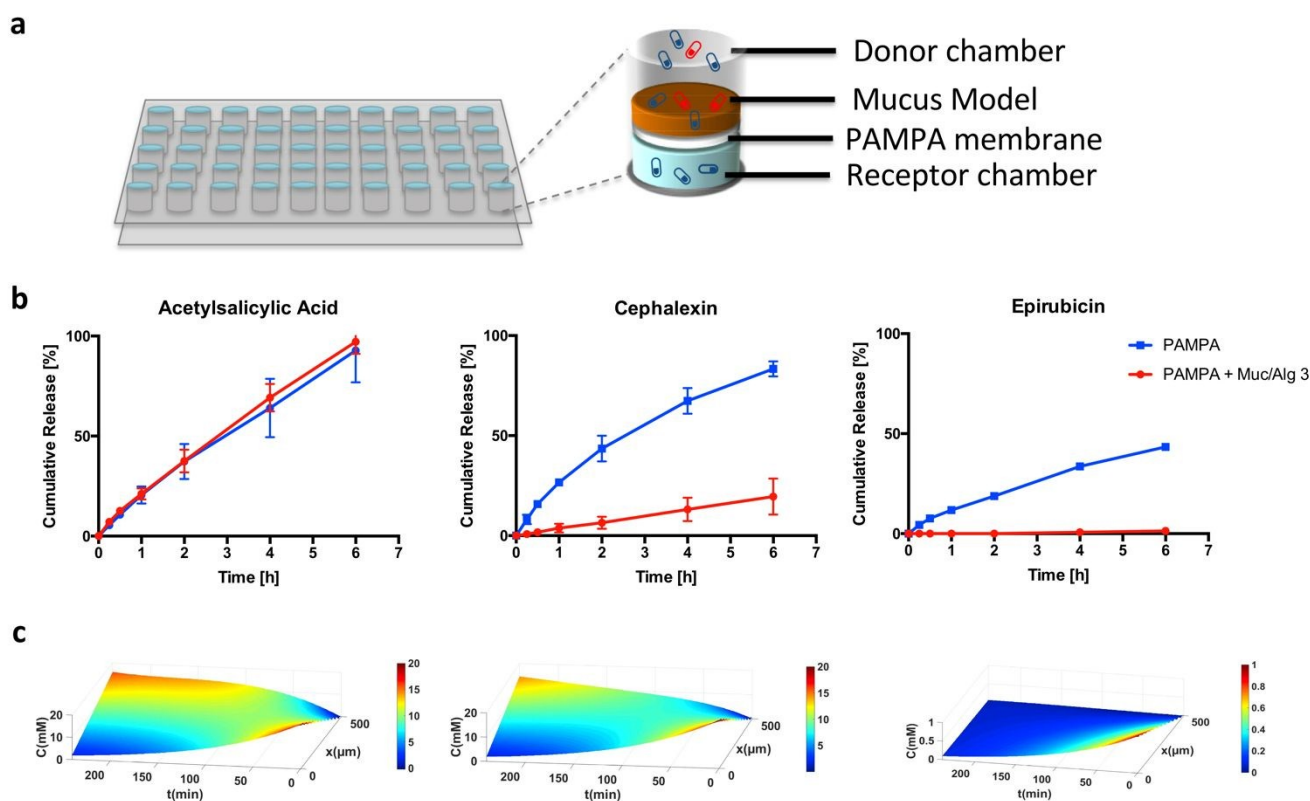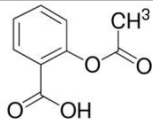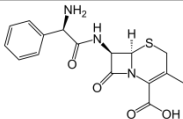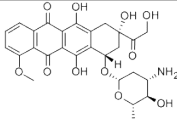
Fig. 6 Drug diffusion tests through the developed airway mucus model. (a) Drug diffusion experimental setup; (b) Cumulative release of acetylsalicylic acid, cephalexin and epirubicin through the empty PAMPA plate (blue line) and in the presence of Muc/Alg 3 hydrogels (red line); and (c) Mathematical model of the diffusion profile of the different drugs within the mucus model.

Table 1. Mesh size (ξ) and Shear Modulus (G) after fitting the GMM on the obtained rheological data of the developed mucus models.

	Alg 2	Muc/Alg 2	Alg 3	Muc/Alg 3	Alg 5	Muc/Alg 5
Estimated ξ (nm) $\pm$ SD	53.7 ± 3.14	75.7 ± 1.67	50.7 ± 8.06	54.7 ± 5.35	42.9 ± 5.68	42.3 ± 1.21
G (Pa) $\pm$ SD	51.5 ± 8.66	18.1 ± 1.23	92.5 ± 27.2	49.3 ± 14.3	110 ± 18.0	104 ± 8.95

Table 2. Physicochemical features of acetylsalicylic acid (ASA), cephalexin and epirubicin. References are added for the data derived from previous work, while all the other data are original data obtained in this work.

	Acetylsalicylic acid	Cephalexin	Epirubicin
Chemical Structure			
Molecular Weight (g/mol)	180.159 [69]	347.389 [70]	543.529 [71]
Charge at pH 7.4*	100% negative	60% negative 40% zwitterion	80% positive 20% zwitterion
Water Solubility (mg/ml)	4.60 [69]	1.79 [70]	0.0930 [71]
van der Waals surface area*	246	433	713
Constant of association with mucin (K_a) (M^{-1}) $\times 10^4$	No interaction	0.610 [18]	7.76
Constant of dissociation with mucin (K_d) (M) $\times 10^{-4}$	No interaction	1.64 [18]	0.130
P_{app} through PAMPA membrane (10^{-6} cm/s)	26.6 ± 1.21	14.9 ± 2.50	9.07 ± 2.59
P_{app} through PAMPA membrane + Muc/Alg 3 (10^{-6} cm/s)	25.8 ± 0.762	5.96 ± 2.95	0.640 ± 0.305

* Both molecular weight and van der Waals surface area of acetylsalicylic acid, cephalexin and epirubicin were calculated using MarvinSketch 16.8.15.0 by ChemAxon (https://www.chemaxon.com).